GEOPHYSICAL RESEARCH LETTERS, VOL. 26, NO. 15, PAGES 2347-2350, AUGUST 1, 1999

High Humidities and Subvisible Cirrus Near the Tropical Tropopause

Eric J. Jensen[1], William G. Read[2], John Mergenthaler[3], Brad J. Sandor[4], Leonhard Pfister[1], and Azadeh Tabazadeh[1]

Abstract. Measurements of water vapor from the Microwave Limb Sounder on the Upper Atmospheric Research Satellite show that humidities in the extreme tropical upper troposphere are often near saturation with respect to ice. These high humidity values are supported by the available accurate in situ water vapor measurements near the tropical tropopause. A nearly saturated upper troposphere reduces the outgoing longwave radiative flux at the top of the atmosphere by about 1–2 W-m^{-2} compared to the radiative flux calculated using a standard atmospheric humidity profile. Subvisible cirrus near the tropopause reduce the outgoing longwave radiation an additional few W-m^{-2} as well as increasing the radiative heating near the tropopause. Changes in the humidity frequency distribution in this region of the atmosphere and the associated changes in subvisible cirrus frequency would substantially impact the radiative budget of the tropics.

Introduction

Water vapor is the dominant infrared absorbing gas in the Earth's atmosphere. The relatively small amount of water in the cold upper troposphere has a relatively large impact on the outgoing longwave radiation [*Clough et al.,* 1992; *Udelhoffen and Hartmann,* 1994]. In spite of its importance, the upper tropospheric water vapor concentration has been poorly quantified in the past. Standard radiosonde humidity sensors are notoriously unreliable at temperatures below about –40°C [*Miloshevich and Heymsfield,* 1998; *Anderson,* 1994]. Nadir sounding satellite-borne sensors have provided information about the mid- and lower-tropospheric water vapor concentration, and precise in situ measurements of upper tropospheric H_2O have been made in selected locations during focused measurement campaigns. However, until recently, global statistical information on relative humidity in the extreme upper troposphere has been unavailable.

Standard atmosphere tropical humidity profiles generally assume that the average relative humidity with respect to ice (RHI) in the upper troposphere ranges from about 10–50% [*McClatchey et al.,* 1972]. However, recent measurements have shown that laminar optically thin cirrus are present near the tropical tropopause with very high occurrence frequencies [*Wang et al.,* 1996]. The fact that these cirrus clouds are present much of the time suggests that this region of the atmosphere must frequently be near ice saturation.

[1]NASA Ames Research Center, Moffett Field, CA
[2]Jet Propulsion Laboratory, Pasadena, CA
[3]Lockheed-Martin, Inc. Menlo Park, CA
[4]National Center for Atmospheric Research, Boulder, CO

Paper number 1999GL900266.
0094-8627/99/1999GL900266$05.00

In this report, we present upper tropospheric humidity measurements from the Microwave Limb Sounder (MLS) on the Upper Atmospheric Research Satellite (UARS). We focus here on the remarkably high humidities observed at the 147 mbar pressure level in the tropics. We show that even cloud-free regions have relatively high humidities near the tropopause. The MLS RHI measurements are supported by comparisons with localized aircraft- and balloon-borne measurements, and a meteorological explanation for the high RHIs near the tropopause is given. The implications of the high humidities for upper tropospheric heating rates and outgoing longwave radiation are evaluated.

MLS Humidity Measurements in the Tropical Upper Troposphere

Retrieval of water vapor from the MLS 205 GHz radiance measurement has been described in detail elsewhere [*Read et al.,* 1995]. The limb-scanning geometry allows retrieval of water vapor concentration on pressure levels of 147, 215, 316, and 464 mbar with vertical weighting functions about 3 km wide. Globally, 1318 individual profiles are measured per day, providing excellent geographic coverage. For this study, we are using version 490 of the MLS RHI retrieval. RHI values are calculated by using the MLS water vapor concentrations and temperatures taken from the National Centers for Environmental Prediction (NCEP) analyses.

MLS has an advantage over other water vapor remote sensing instruments in that it can retrieve water vapor even when clouds are present. However, the retrieval is not en-

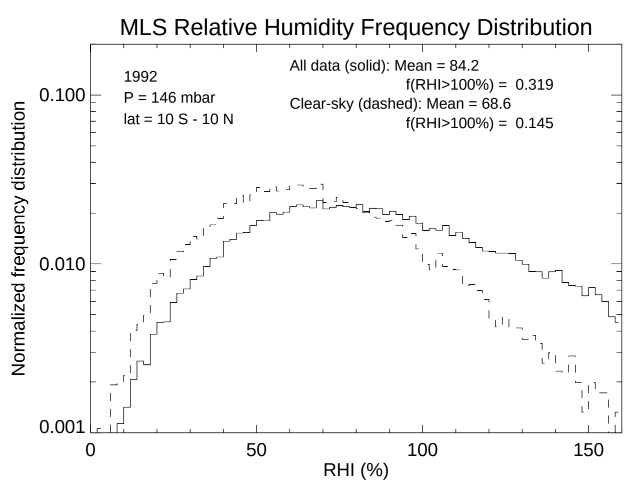

Figure 1. Frequency distributions of RHI based on MLS data from 1992 at 146 mbar restricted to latitudes equatorward of 10°. Solid curve: All data; dashed curve: only data points for which the corresponding CLAES extinction was less than 0.001 km^{-1} (i.e., cloud-free).

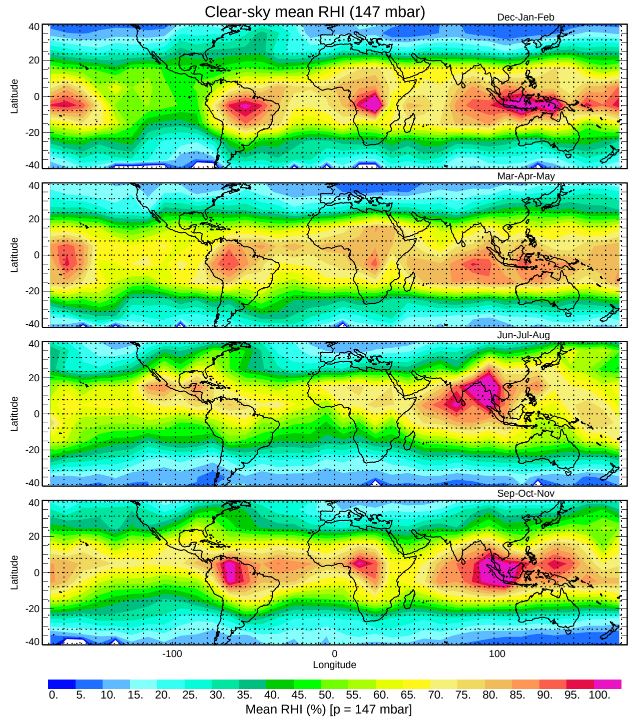

Figure 2. Seasonal maps of the mean RHI at 146 mbar calculated from the cloud-free 1992 MLS data. The mean humidities are relatively high throughout the tropics.

tirely insensitive to clouds. The instrument is about a factor of 2 less sensitive to ice than to water vapor per mass. Hence, some of the retrieved RHI values in excess of 100% may be due to cloud contamination. Fortunately, the infrared extinction measurements from the Cryogenic Limb Array Etalon Spectrometer (CLAES) co-aligned with MLS on the UARS satellite provide a very sensitive cloud detection measurement [*Mergenthaler et al.,* 1998]. The CLAES measurements have been used for validation of the MLS RHI retrievals [B. Read, personal communication]. We use the CLAES extinctions here to determine which MLS measurements were taken with clouds along the line of sight.

Figure 1 shows the frequency distribution of MLS RHI values at 147 mbar from 1992 for latitudes equator-ward of 10°. This dataset consists of 111,950 individual measurements. The mean RHI from this dataset is 78%, which is remarkably high compared to values of 5–20% typically reported for lower levels [*Sandor et al.,* 1998; *Spencer and Braswell,* 1997; *Chiou et al.,* 1997]. Also, a large fraction (28%) of the measurements indicated supersaturation with respect to ice (RHI > 100%) at the 147 mbar level in the tropics. The dashed curve in Figure 1 shows the result of restricting the dataset to MLS measurements for which the corresponding CLAES measurement indicated extinction (along the limb) less than 0.001 km^{-1}. This restriction should provide a cloud-free dataset (even subvisible cirrus should be removed). About 70% of the data points are excluded by using this extinction threshold. The mean RHI is reduced to 66%, and the fraction of measurements with RHI > 100% is reduced considerably to 14%. However, even with this clear-sky dataset, the mean humidities at the 147 mbar level are still much higher than at lower levels in the troposphere.

The large random error in the MLS RHI retrieval will tend to broaden these frequency distributions. Hence, some of the values > 100% could be regions that were near saturation and the retrieval gave an anomalously high value. To quantitatively assess this problem we assume that the true distribution of cloud-free RHIs can be represented by the MLS clear-sky values if we exclude RHIs greater than 100%. Next, we add random errors (with a standard deviation of 20%) to these assumed true values. The resulting distribution of RHIs has about 8% of its values greater than 100%. Hence, random errors probably do contribute substantially to the number of retrievals with RHI > 100%. In contrast, the average humidity should not be changed dramatically by the random errors.

Another source of error in the MLS RHI retrieval is the uncertainty in NCEP temperatures. Radiosonde measurements are sparsely distributed throughout the tropics; hence, the accuracy of the analyses depends upon how well the meteorological model represents atmospheric processes. Even if the analysis temperatures are randomly distributed around the true temperature, the non-linearity in the Clausius-Clapyron relation for saturation vapor pressure results in a high bias in the mean RHI. A 2 K random error in the analysis temperatures would bias the mean RHI by a few %. A 4 K random error would bias the mean RHI more than 12%.

Another important issue here is the relatively large footprint of the MLS measurement. Given the limb-scanning geometry and the field of view of MLS, each measurement is essentially an average over a horizontal area of about 100x200 km^2 and a vertical distance of about 3 km. Lidar measurements of water vapor have shown that high humidities are often present in narrow laminae in the upper troposphere [*Newell et al.,* 1996]. These small-scale regions of high humidity will be averaged with surrounding lower humidity regions by the MLS sampling. In other words, the frequency distribution of RHI measurements would be

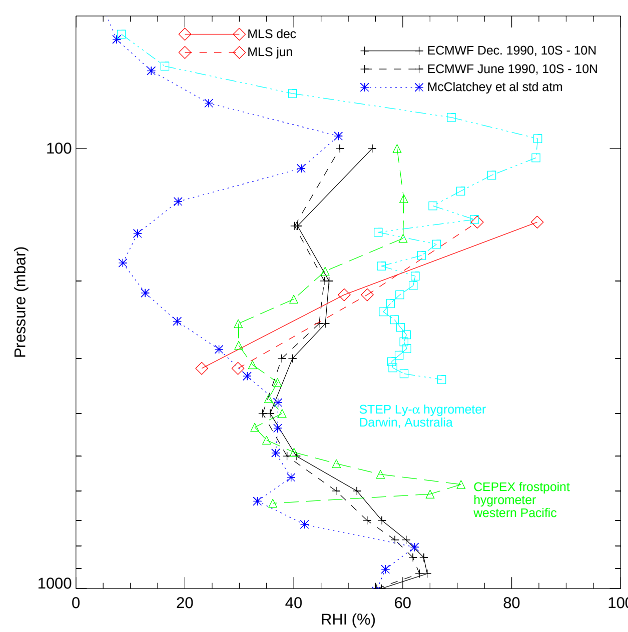

Figure 3. Average RHI height profiles are shown from MLS, ECMWF, STEP, and CEPEX measurements (see text for discussion).

Table 1. Radiative Transfer Model Results

Model Atmosphere	OLR[a]
ECMWF[b]	300.9
MLS[c]	299.5
MLS and laminar cirrus cloud[d]	295.9
ECMWF, dry below 200 mbar	313.6
MLS, dry below 200 mbar	309.7

[a]Upwelling longwave radiative flux (W-m^{-2}).
[b]Water vapor profile fit to the ECMWF July mean profile.
[c]Water vapor profile fit to the annual average MLS values at 316, 215, and 147 mbar.
[d]Subvisible, laminar cirrus cloud placed at 16–16.5 km (see text).

broader if measurements with higher spatial resolution were used.

In summary, the frequency distribution of RHI values retrieved by MLS is broader than the true distribution due to random errors, but the MLS distribution may be narrower than the true distribution due to the broad spatial averaging. However, if these errors are random and the temperature uncertainty is no larger than about 2 K, then the mean RHIs calculated from the MLS data should be accurate to within a few %.

Figure 2 shows the seasonal and geographic distribution of average RHI at 147 mbar based on all MLS measurements from 1992 for which the CLAES extinction was less than 0.001 km^{-1}. The mean RHI ranges from about 50% to $>$ 100% in the deep tropics. The peak values correspond to regions with strong convection and regions with high frequency of subvisible cirrus [*Wang et al.,* 1996]. However, even in the descending branches of the Walker-cell circulation (eastern Pacific and west of Africa), the mean RHI is still greater than 50%. The high humidities throughout the tropics are consistent with observations of thin cirrus near the tropopause even in regions dominated by descent through most of the troposphere [*Winker and Trepte,* 1998].

The vertical profile of tropical clear-sky RHI from MLS is compared to averages predicted by the European Center for Medium Range Weather Forcasts (ECMWF) meteorological analysis model in Figure 3. Due to the uncertainties of radiosonde humidity measurements at low temperatures, the ECMWF analyses do not use humidity values reported at pressures below 250 mbar; hence, the RHIs predicted by the analyses at lower pressures are based on model predictions and must be considered uncertain. The average humidities at the MLS 215 and 316 mbar levels agree reasonably well with the ECMWF values. However, at 147 mbar, the MLS retrieval indicates much higher RHIs than the analysis. The discrepancy would be even larger if we included all of the MLS data in the averages (measurements with clouds as well as the clear-sky data). Also shown in Figure 3 is the *McClatchey et al.* [1972] standard tropical humidity profile. This profile has been used in radiative transfer intercomparison studies [e.g., *Ellingson and Fouquart,* 1991]. Just like the ECMWF mean profiles, the McClatchey et al. standard atmosphere specifies humidities well below the MLS measured humidities in the extreme upper troposphere.

The high humidities in the tropical upper troposphere indicated by the MLS retrieval are supported by the limited number of in situ water vapor measurements made with accurate water vapor sensors. Figure 3 shows average water vapor vertical profiles made with a frost-point hygrometer mounted on balloons and a Lyman-alpha hygrometer onboard the ER-2 aircraft during focused field experiments in the tropics. The 13 frost-point hygrometer soundings were taken during springtime as part of the Central Equatorial Pacific Ocean Experiment (CEPEX) in the central-western Pacific [*Kley et al.,* 1996; *Vömel et al.,* 1995] where the MLS data suggests mean RHI values of 60–90% at 147 mbar. The ER-2 measurements from the Stratosphere-Troposphere Exchange Project (STEP) are 16 descents at Darwin, Australia [*Kelly et al.,* 1993] where MLS indicates RHI values of 70–90%. These in situ measurements generally showed high RHIs near the tropopause, in agreement with the MLS data.

From a thermodynamic point of view, high humidities in the upper tropical troposphere should not be surprising. The tropical tropospheric circulation is characterized by strong upward motion in the small portion of the tropical atmosphere that contains convective systems, and slow descent in the large regions free of deep convection. This slow descent is consistent with the radiation budget in the clear areas, which shows substantial radiative cooling maximizing at about 1.75 K-day^{-1} at 400 mb. Above about 150 mb, however, there is mean radiative heating, with a maximum value of about 0.5 K-day^{-1} at the tropopause. This heating is largely due to the very cold temperatures in extreme upper tropical troposphere. The presence of laminar, subvisible clouds near the tropopause actually enhances this heating.

To maintain a steady-state temperature in the nonconvective areas of the atmosphere, these radiative heating rates suggest that there exists a mean downward motion below 150 mb, and upward motion above. Given that tropical convective systems have their largest detrainment between 350 and 100 mb [*Houze,* 1989], most of the air at these altitudes in tropical clear areas is probably convective outflow with humidities near ice saturation. One expects that the relative humidity of air below 150 mb will decrease rapidly as the air descends and warms, while the relative humidity of air above 150 mb will rise slowly or remain near saturation.

Implications for Cloud Formation and Radiation Budgets

The high humidities in the tropical tropopause region are no doubt closely related to the frequent occurrence of cirrus clouds in this region. With large-scale RHI values on the order of 80–100%, even lifting (cooling) of air parcels by only a few hundred meters will be sufficient to supersaturate the air leading to ice nucleation and growth. The slow lifting which maintains the high humidities in the extreme upper troposphere also promotes the formation and persistence of subvisible cirrus.

As discussed above, water vapor in the upper troposphere is an important greenhouse gas. Radiative transfer calculations have suggested that 10% changes in the RHI result in changes in the outgoing longwave flux (OLR) of about 0.5–1.4 W-m^{-2} [*Udelhofen and Hartmann,* 1995]. To further assess the radiative impact of the high humidities near the tropopause suggested here, we have used a 4-stream radiative transfer code. A standard atmosphere temperature profile is used with a surface temperature of 300 K and a tropopause temperature of 194.8 K. The surface albedo is set to 0.07. Table 1 lists the OLR values calculated using humidity profiles fit to the tropical average ECMWF data (red curves) and the MLS data (green curves). Using the higher RHI values indicated by MLS rather than the ECMWF averages results in a decrease in the OLR from 300.9 to 299.5 W-m^{-2}. The higher RHI values cause decreases in solar heating rates of about 0.1–0.2 K-day^{-1} between 12 and 20 km and similar magnitude decreases in IR cooling rates.

The impact of water vapor near the tropopause is even more pronounced in subsidence regions where air is very dry throughout the free troposphere below about 200 mbar. It has been suggested that these arid regions dominate the radiative energy escape from the tropics [*Pierrehumbert,* 1995]. Assuming an RHI of 10% in the free troposphere below 200 mbar, increasing the RHI in the 100–200 mbar layer from 50% to 100% results in a decrease in the OLR by about 4 W-m^{-2} (see Table 1).

We have also run the radiative transfer model with a thin subvisible cirrus cloud at 16 km. Based on measurements of laminar cirrus near the tropopause [*Heymsfield et al,* 1986], the ice crystal size distribution in the cloud is represented by a log-normal distribution with a number density of 1 cm^{-3}, a mode radius of 3.5 μm, and a standard deviation of 1.2. The corresponding ice water content is about 0.2 mg-m^{-3} (1.6 ppmv at 16 km) which is a small fraction of the water vapor at this level (about 10 ppmv). The cloud vertical depth is 500 m, resulting in a zenith visible optical depth of 0.02. The cloud causes a sharp layer with radiative heating of about 3 K-day^{-1} and a further decrease in the OLR from 299.5 to 295.9 W-m^{-2}. The cloud radiative heating will drive a combination of local temperature increase, upward vertical motion of the cloud [*Rosenfield et al.,* 1998], and turbulent motions in the cloud. The relative magnitude of these effects will depend strongly upon the horizontal scale of the cloud and the temperature lapse rate.

The frequency of occurrence of cirrus clouds detected by SAGE II and CLAES in the top few kilometers of the tropical tropopause, averaged over latitudes 10 S to 10 N, is about 40-50% [*Wang et al.,* 1996]. Most of these clouds are subvisible and highly laminar [*Winker and Trepte,* 1998]. The radiative forcing of these clouds is only a few W-m^{-2}, which is more than an order of magnitude lower than the cloud forcing due to other types of cirrus [Hartmann et al., 1992]; however, their high areal coverage implies that they are a substantial perturbation to the tropical radiation budget, and they can have a large impact on the heat budget near the tropopause.. The occurrence frequency of these clouds depends upon several factors including the frequency distribution of RHI in the upper troposphere, the magnitude and frequency of dynamical perturbations such as Kelvin waves and gravity waves, and the critical supersaturation required to initiate ice nucleation (which depends upon the aerosol composition).

The net radiative impact of the high humidities and cirrus depends very sensitively on how much of the H_2O mass is condensed. Future changes in the occurrence frequency or optical properties of these clouds could be an important factor in the climate evolution. Hence, it is important to better understand the processes controlling water vapor and cloud formation in this region of the atmosphere.

Acknowledgments. This research was supported by NASA's Upper Atmospheric Research Sattelite Interdisciplinary Research Program, directed by Robert McNeal.

References

Anderson, P. S., A method for rescaling humidity sensors at temperatures well below freezing, *J. Atmos. Oc. Tech., 11*, 1388, 1994.

Chiou, E. W., M. P. McCormick, and W. P. Chu, Global water vapor distributions in the stratosphere and upper troposphere derived from 5.5 years of SAGE II observations (1986–1991), *J. Geophys. Res., 102*, 19105, 1997.

Clough, S. A., et al., Line-by-Line calculations of atmospheric fluxes and cooling rates: Application to water vapor, *J. Geophys. Res., 97*, 15761, 1992.

Ellingson, R. G., and Y. Fouquart, The intercomparison of radiation codes in climate models: An overview, *J. Geophys. Res., 96*, 8925, 1991.

Hartmann, D. L., et al., The effect of cloud type on Earth's energy balance: Global analysis, *J. Climate, 5*, 1281, 1992.

Heymsfield, A. J., et al., Ice particles observed in a cirroform cloud at –85°C and implications for polar stratospheric clouds, *J. Atmos. Sci., 43,* 851–855, 1986.

Houze, R. A., Observed structure of mesoscale convective systems and implications for large-scale heating, *Q. J. R. Meteorol. Soc., 115*, 425, 1989.

Kley, D., et al., Observations of near-zero ozone concentrations over the convective Pacific: effects on air chemistry, *Science, 274*, 230, 1996.

Kelly, K., A. F. Tuck, and T. Davies, Wintertime asymmetry of upper tropospheric water between the Northern and Southern Hemispheres, *J. Geophys. Res., 98*, 8713, 1993.

McClatchey et al., Optical properties of the atmosphere, *Environ. Res. Pap., AFCRL-72-0497*, Air Force Cambridge Res. Lab., Bedford, Mass., 1972.

Mergenthaler et al., Observations of Tropical Cirrus by CLAES, in preparation, 1998.

Miloshevich, L. M., and A. J. Heymsfield, Undermeasurement of high relative humidities in the upper troposphere by vaisala RS80-A radiosondes, presented at the *10th Symposium on Meteorological Observations and Instrumentation*, 11–16 Jan., Phoenix, Arizona, 1998.

Newell, R. E. et al., Upper tropspheric water vapor and cirrus: Comparison of DC-8 observations, preliminary UARS microwave limb sounder measurements and meteorological analyses, *J. Geophys. Res., 101*, 1943, 1996.

Pierrehumbert, R. T., Thermostat, radiator fins, and local runaway greenhouse, *J. Atmos. Sci., 52*, 1784, 1995.

Read, W. G. et al. Upper-tropospheric water vapor from UARS MLS, *Bull. Am. Meteorol. Soc., 76*, 2381–2389, 1995.

Rosenfield, et al., The impact of subvisible cirrus clouds near the tropical tropopause on stratospheric water vapor, *Geophys. Res. Lett., , 25*, 1883–1886, 1998.

Sandor, B., et al., Seasonal behavior of tropical to mid-latitude upper tropospheric water vapor from UARS MLS, *J. Geophys. Res., 103*, 25935, 1998.

Spencer, R. W., and W. D. Braswell, How dry is the tropical free troposphere? Implications for global warming theory, *Bull. Am. Meteorol. Soc., 78*, 1097–1106, 1997.

Udelhoffen, P. M., and D. L. Hartmann, Influence of tropical cloud systems on the relative humidity in the upper troposphere, *J. Geophys. Res., 100*, 7423–7440, 1994.

Vömel, H., et al., New evidence for the stratospheric dehydration mechanism in the equatorial Pacific, *Geophys. Res. Lett., , 22*, 3235, 1995.

Wang, P.-H. et al., A 6-year climatology of cloud occurrence frequency from Stratospheric Aerosol and Gas Experiment II observations, *J. Geophys. Res., 101*, 29407, 1996.

Winker, D., and C. Trepte, Laminar cirrus observed near the tropical tropopause by LITE, *Geophys. Res. Lett. 25*, 3351, 1998.

Eric. J. Jensen, NASA Ames Research Center, MS 245-4, Moffett Field, CA 94035.

(Received October 16, 1998; revised December 17, 1998; accepted December 22, 1998.)